Geometrico-Static Modelling of a FRE Finger

Peng Wang, Vincent Bégoc, and Sébastien Briot

Abstract This article presents a discrete geometrico-static model for a Fin-Ray Effect (FRE) finger capable of predicting both deformation and contact forces during grasping. The finger is modeled as two Cosserat rods interconnected by rigid lamellae and flexible hinges, the latter being modeled as Cosserat rods as well. The equilibrium configuration is obtained by minimizing the potential energy subject to nonlinear loop-closure and contact constraints. Validation against finite element analysis (FEA) and experiments shows that the proposed model provides comparable accuracy to FEA in terms of predicted geometry and contact forces, while requiring significantly less computation time. The approach thus offers an efficient alternative to FEA for the analysis and design optimization of FRE fingers.

1 Introduction

The Fin-Ray-Effect (FRE) finger, originally introduced in [6], is a closed-chain continuum mechanism inspired by the structure of fish fins. Its V-shaped compliant configuration allows passive adaptation to an object with-

P. Wang
École Centrale de Nantes, Laboratoire des Sciences du Numérique de Nantes (LS2N), UMR CNRS 6004, Nantes, France
Harbin Institute of Technology (HIT), School of Mechatronics and Engineering, China
e-mail: Peng.Wang@ls2n.fr

V. Bégoc
École Centrale de Nantes and Institut Catholique d'Arts et Métiers (Icam)
e-mail: vincent.begoc@icam.fr

S. Briot
Laboratoire des Sciences du Numérique de Nantes (LS2N), UMR CNRS 6004, Nantes, France, and Centre National de la Recherche Scientifique (CNRS)
e-mail: Sebastien.Briot@ls2n.fr

out complex actuation or sensing. This simplicity has made FRE fingers attractive for safely manipulating fragile and irregular items. However, since adaptation results from the intrinsic structure rather than active control, the grasping performance depends on the finger's geometry and its material properties which motivates the need for mathematical models capable of predicting both the deformed configuration of the finger and the resulting contact forces.

Several modelling strategies have been explored to address this problem. Finite-element analysis (FEA) has been widely used due to its generality and accuracy, and is frequently employed as a benchmark or as a tool for structural optimization [2, 3]. However, FEA simulations are computationally expensive, making it difficult to optimize the design of such finger over a large design space.

Alternative approaches have been proposed using the virtual-work principle to obtain a kinetostatic model [7], or Cosserat-rod theory to model the finger as a closed-chain of Cosserat rods [1, 8]. However, in these works, the contact forces must be prescribed to obtain the deformed shape. In [10, 11], each rod is discretized as a chain of cantilever beams using the Beam Constraint Model, enabling the computation of the configuration minimizing the strain energy and contact forces. Despite its interest, these works are not applicable to Festo-like fingers, since they do not consider flexible hinges between the front/back beams and the lamellae, despite their strong influence on the transmission of contact forces as analysed in [7].

In this work, we propose a discrete geometrico-static model that jointly computes the contact configuration of the finger and the contact forces. The front and back beams are modeled as Cosserat rods, as well as the flexible hinges connecting beams to rigid lamellae. The equilibrium configuration is obtained by minimizing the total potential energy of the finger subject to nonlinear loop-closure and contact constraints, formulated respectively as equalities and inequalities and solved using an active-set strategy [5]. All model parameters derive directly from geometry and material properties, and beams. Below, we evaluate the accuracy of this model in estimating the shape and contact forces, through comparison with finite element simulations and experimental measurements.

2 Geometrico-static Modelling

2.1 FRE-finger description and modelling hypotheses

The Festo FRE-finger (Fig 1) can be decomposed as follows:

- the **front beam** in contact with the grasped object
- the **back beam**

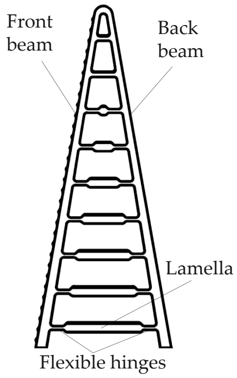

(a) Full finger

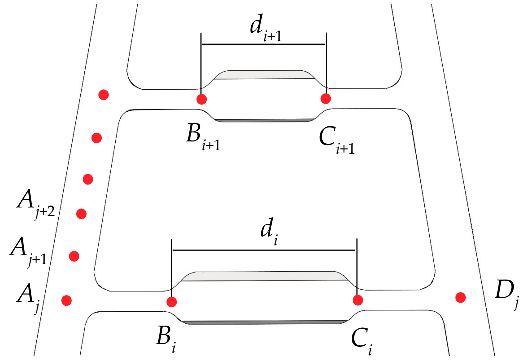

(b) Zoomed view

Fig. 1 Scheme of the Festo FRE-finger

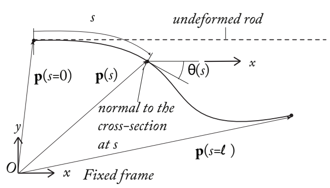

(a) Continuous parameterization

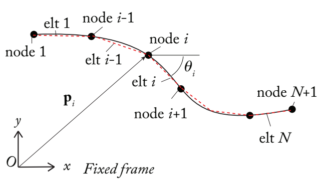

(b) Discrete parameterization

Fig. 2 Parameterization of the flexible rod

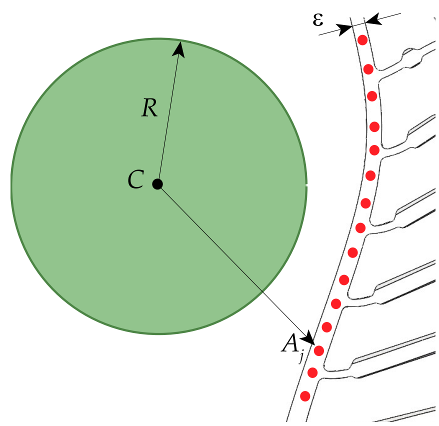

Fig. 3 Contact constraints of the FRE-finger

- the **lamellae**. Note that the lamellae is rigidly connected to a revolute motor.
- the **flexible hinges** connecting the front and back beams to the lamellae.

In what follows, the lamellae are modeled as rigid segments since early FEA simulation show low deformation. The front and back beams, and the flexible hinges, showing large deformations, are modelled using Cosserat theory [12].

2.2 Modelling of a flexible rod

We consider an isotropic flexible rod to represent either the front or back beams, or the flexible hinges (Fig. 2(a)). The rod has a uniform or variable cross-section along its curvilinear abscissa ($s \in [0\,\ell]$), where ℓ denotes its total length. Shear and extensibility of the rod are considered as negligible and all deformations are assumed to be in the Oxy plane. Thus, the deformation energy of the rod based on the Cosserat formalism is:

$$V_e = \frac{1}{2}\int_0^{\ell} EI(\theta'(s) - \theta'^*(s))^2 ds \tag{1}$$

with E the material Young's modulus, I the second moment of area of the cross-section, $\theta' = d\theta/ds$ the derivative of the cross-section orientation, and θ'^* the initial value of θ' in the undeformed state.

Following [12], θ' can be approximated using finite-difference. The rod is discretized into N rigid elements of equal length $\ell_e = \ell/N$ (Fig. 2(b)). The segment i (between nodes i and $i+1$) takes an orientation θ_i after deformation. Function $\theta'(s)$ on segment i is approximated as:

$$\theta'(s) \approx (\theta_i - \theta_{i-1})/\ell_e \tag{2}$$

Then, the deformation energy of element i is

$$V_{ei} \approx \frac{1}{2}\frac{EI}{\ell_e}(\theta_i - \theta_{i-1})^2 \tag{3}$$

and the total deformation energy of the rod could be calculated as

$$V_e(\boldsymbol{\theta}) \approx \sum_{i=1}^{N} V_{ei} \tag{4}$$

with vector $\boldsymbol{\theta}$ containing all variables θ_i's.

2.3 Potential energy of the FRE-finger

Based on the previous formalism, the total potential energy of the finger may be expressed as:

$$V(\boldsymbol{\Theta}) = V_F + V_B + \sum_{k=1}^{N_H} V_{Jk} \tag{5}$$

where V_F, V_B are the deformation energy of the Front and Back beams resp., V_{Jk} is the deformation energy of the k-th flexible hinge, N_H being the total number of hinges, and vector $\boldsymbol{\Theta}$ groups all configuration variables θ_i for all Cosserat beams.

2.4 Model of the FRE-finger during contact

The configuration $\boldsymbol{\Theta}$ of the finger during contact can be computed by minimizing the potential energy of the finger (5), subject to some geometric constraints:

- Internal constraints (equality constraints):
  - Since lamellae are rigid, the distance between hinges extremities at B_i and C_i must be constant (Fig. 1(b)). Additionally, the orientation of the hinges at these points must be equal to the orientation of the lamella.
  - The other extremities of the hinges being rigidly connected to either the front or back beams, at points A_j or D_j (Fig. 1(b)), the changes of positions and orientations of the hinges at these points must be equal to the changes of positions and orientations of the back and front beams at the connection points.

  These equality constraints are stacked in a function $\boldsymbol{h}(\boldsymbol{\Theta}) = \mathbf{0}$
- External constraints (inequality constraints): they characterize the potential contact between the grasped object and the front beam. In this paper, we consider a cylindrical object whose axis is directed along $\mathbf{z}$ (normal to the plane Oxy). To avoid interpenetration between the finger and the cylinder, the following constraints must be respected:

$$\left\| \overrightarrow{A_j C} \right\|_2 - r \geqslant 0, \qquad (\forall j = 1, \cdots N_A) \tag{6}$$

  where, A_j is the j-th node on the discretized front beam, N_A is the number of elements of the front beam, C the center of the cylinder's cross-section, and $r = R + \epsilon/2$, R being the cylinder radius, and ϵ the thickness of the front beam (Fig. 3). All these non-penetration inequality constraints are stacked in a function $\boldsymbol{g}(\boldsymbol{\Theta}) \leq \mathbf{0}$.

The configuration of the finger $\boldsymbol{\Theta}$ when grasping an object, can be found by solving the following optimization problem using an interior-point strategy [5]:

$$\begin{aligned} &\min_{\boldsymbol{\Theta}} V(\boldsymbol{\Theta}) \\ s.t. \quad &\boldsymbol{g}(\boldsymbol{\Theta}) \leq \mathbf{0} \\ &\boldsymbol{h}(\boldsymbol{\Theta}) = \mathbf{0} \end{aligned} \tag{7}$$

Note that the contact forces applied by each element of the front beam on the cylinder can be rebuilt once the problem (7) is solved, by extracting the Lagrange multipliers associated with the inequality constraints $\boldsymbol{g}(\boldsymbol{\Theta}) \leq \mathbf{0}$ [9].

Cylinder diameter	Contact height	$\alpha_1(°)$	α_2	α_3	α_4
$80\,mm$	High	11	13	15	17
	Mid	12	15	17	19
	Low	13	15	17	19
$60\,mm$	High	18	20	22	24
	Low	22	24	26	28

Table 1 Motor angles for each contact case with respect to the y-axis

3 Experimental Assessment of Model Accuracy

An instrumented experimental benchmark was developed to replicate the interaction between a FRE finger and a cylindrical object, enabling systematic evaluation under varying conditions. The section first presents the benchmark architecture and instrumentation, and give details on the FEA. We then compare the discrete model and FEA simulations with experimental results in order to assess their ability to predict finger deformation and contact forces.

3.1 Experimental Benchmark

The proposed benchmark (Fig. 4) consists of a FRE finger (manufactured by Festo, ref. DHAS-GF-80-U-BU [4]), actuated in rotation and grasping a cylindrical object. The first lamella of the finger is rigidly attached to a servo-motor through a custom mechanical interface. The motor (Dynamixel XM430-W350-T) is controlled in position.

Finger configuration was captured using a camera and MATLAB-based vision algorithm [13]. MATLAB evaluation yielded calibration mean/max errors of 0.06/0.12 pixels ($\pm 0.85/\pm 1.14 \mu m$ in the measured plane). The contact force exerted by the finger on the object is measured along the $\mathbf{x}$ and $\mathbf{y}$ directions using two force sensors (SBT-620, SIMBATOUCH, with a precision of ± 0.02 N). The cylindrical object is connected to the force measurement system via a revolute joint, enabling free rotation about the $\mathbf{z}$ axis. This setup reproduces near-frictionless contact conditions between the finger and the object.

To evaluate the proposed model under a wide range of conditions, multiple contact configurations have been evaluated, combining the following parameters:

- **Cylinder diameters**: $60\,mm$ and $80\,mm$,
- **Contact heights**: three positions labeled “High”,“Mid”, and “Low” (Fig. 5);
- **Motor angles**: four discrete angle inputs, labeled α_1 to α_4 (Tab. 1).

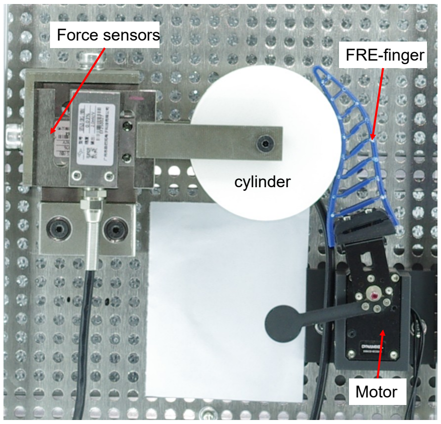

Fig. 4 Instrumented benchmark used for experiments equipped with a Festo FRE finger actuated by a rotating motor, a grasped cylinder and force sensors.

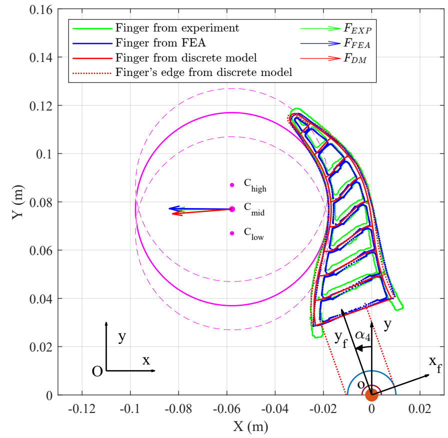

Fig. 5 Comparison of deformed finger geometry from experiments (green), FEA simulations (blue) and discrete model (red), and the corresponding net contact forces.

3.2 FEA details

FEA simulations were conducted using the nonlinear static module of the SOLIDWORKS Simulation software in order to account for large deformations. The FRE-finger CAD file supplied by FESTO was imported into the simulation. FESTO provides limited material property data for the DHAS finger, specifying only that they are fabricated from **thermoplastic polyurethane (TPE-U)** [4]. A Young's modulus of $E = 4.95 \times 10^7$ Pa was used for both FEA and the discrete model, minimizing the error between FEA and experimental results. (Some key FEA settings: Blended curvature-based mesh (second-order) with minimum/maximum element sizes 0.1/4 mm, surface-to-surface contact model, and large displacement formulation.)

3.3 Comparison Results

The predictions of the discrete model and FEA simulations were evaluated against experimental measurements using two complementary metrics:

- **Geometric accuracy**: the minimal and maximal deviation (in mm) along the $\mathbf{x}_f$ direction (Fig. 5), between the predicted finger geometry and the experimentally measured geometry.
- **Contact force accuracy**: the error (in Newton) between the predicted and the measured net contact force amplitudes (Fig. 5).

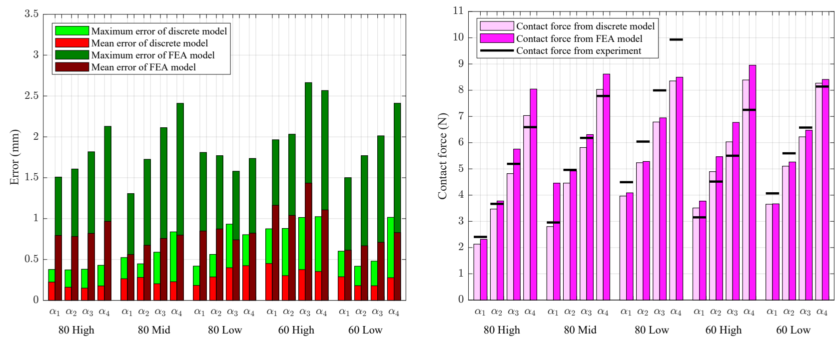

(a) Geometric prediction (b) Contact force prediction

Fig. 6 Comparison of geometry and contact force predictions for various cases.

For geometric predictions (Fig. 6(a)), the discrete model achieves high accuracy across all tested cases, with mean and maximal positional errors along the finger's front beam of 0.45 mm and 1.02 mm, outperforming the present FEA model in the tested cases, whose mean and maximal errors are 1.43 mm and 2.66 mm. For contact force predictions (Fig. 6(b)), both the discrete model and FEA simulations exhibit comparable accuracy, with maximum deviations of 15.8% and 23.4% relative to experimental measurements, respectively.

In terms of computational efficiency, the discrete model completes a simulation in 2–3 seconds, whereas the present FEA model requires 30–60 minutes under similar conditions. The optimization problem was solved using an interior-point algorithm with analytical gradients and Hessians for faster convergence. The number of discretization variables was tuned to balance accuracy and computation time (170 elements per beam and 20 elements per flexible hinge).

4 Conclusion

In this paper, we present a geometrico-static modeling approach for the FRE finger based on finite-difference approximations. Equilibrium configurations are obtained by minimizing the finger's deformation energy under geometric and contact constraints. The model accuracy is verified experimentally and via FEA simulations across multiple contact scenarios. Results show that the discrete model reliably predicts equilibrium configurations, with mean and maximum geometric errors of 0.45 mm and 1.02 mm, respectively. For contact force predictions, it achieves accuracy comparable to the present FEA model, with a maximum deviation of 15.8% relative to measurements. The discrete model is computationally efficient, finishing simulations in a few seconds, while the present FEA model requires 30–60 minutes.

Future work will examine the estimated contact-force distribution and use the proposed model to optimize finger design for improved grasping performance.

References

1. Armanini, C., et al.: Discrete Cosserat Approach for Closed-Chain Soft Robots: Application to the Fin-Ray Finger. IEEE Trans. Robot. **37**(6), 2083–2098 (2021)
2. Crooks, W., et al.: Passive gripper inspired by Manduca sexta and the Fin Ray® Effect. Int. J. Adv. Robot. Syst. **14**(4) (2017)
3. Elgeneidy, K., et al.: Characterising 3D-printed Soft Fin Ray Robotic Fingers with Layer Jamming Capability for Delicate Grasping. In: IEEE RobotSoft, pp. 143–148 (2019)
4. Festo: Adaptive gripper finger DHAS (2024). URL https://www.festo.com/us/en/a/3998964/
5. Nocedal, J., Wright, S.: Numerical Optimization. Springer (2006)
6. Pfaff, O., et al.: Application of FinRay Effect approach for production process automation. In: Proc. 22nd Int. DAAAM Symp., vol. 22. Vienna, Austria (2011)
7. Shan, X., Birglen, L.: Modeling and analysis of soft robotic fingers using the fin ray effect. Int. J. Robotics Res. (2020)
8. Sofla, M.S., et al.: Modeling and modification of fin-ray effect grippers to improve their load capacity and grasp stability. Sens. Actuators A: Phys. **392** (2025)
9. Wriggers, P.: Computational Contact Mechanics. Springer, Berlin, Heidelberg (2006)
10. Yao, J., et al.: Design optimization of soft robotic fingers biologically inspired by the fin ray effect with intrinsic force sensing. Mech. Mach. Theory **191** (2024)
11. Yao, J., et al.: Modeling and performance analysis of a trapezoidal section beam for soft robotic fingers using the fin ray effect. Mech. Mach. Theory **199** (2024)
12. Zaccaria, F., et al.: An Analytical Formulation for the Geometrico-Static Problem of Continuum Planar Parallel Robots. In: ROMANSY 23, pp. 512–520. Springer (2021)
13. Zhang, Z.: A flexible new technique for camera calibration. IEEE Transactions on Pattern Analysis and Machine Intelligence **22**(11), 1330–1334 (2000). DOI 10.1109/34.888718